Petroleum Science 23 (2026) 2275–2287

Contents lists available at ScienceDirect

Petroleum Science

journal homepage: www.keaipublishing.com/en/journals/petroleum-science

Original Paper

Analysis of solidification process and gas sealability of Sn58Bi alloy plugging casing

Chun-Qing Zha, Wen-Chao Tao*, Gong-Hui Liu, Wei Wang

Beijing University of Technology, Beijing, 100124, China

ARTICLE INFO

Article history:
Received 27 October 2024
Received in revised form
16 September 2025
Accepted 23 November 2025
Available online 27 November 2025

Edited by Teng Zhu and Min Li

Keywords:
Sn58Bi alloy plug
Expansion force
Sealing integrity
Casing-plug materials

ABSTRACT

The Sn58Bi alloy plug, composed of 58% bismuth (Bi) and 42% tin (Sn), emerges as a promising alternative to conventional cement plugs. Investigating its mechanical behavior throughout the molten-to-solidified transition is crucial for predicting its performance in downhole oil and gas applications. Particular emphasis was placed on characterizing early expansion behavior during solidification, as the magnitude of expansion force directly correlates with sealing integrity. To analyze temperature and expansion force dynamics during plug formation, a specialized experimental apparatus was developed. Expansion and sealing integrity tests revealed three key findings: Applying overlying axial pressure (0–2 MPa) significantly enhanced plug sealing capacity, with a linear relationship observed between sealing performance and pressure magnitude. In addition, slower and more uniform cooling facilitated expansion both radially and at the axially constrained bottom. Increasing the length-to-diameter ratio (L/D) of 2–6 induced sequential solidification patterns, wherein final-stage solidification drove radial expansion of residual molten alloy, thereby improving gas sealing integrity. These findings establish a theoretical framework for the application of Sn58Bi alloy as downhole casing-plug material.

1. Introduction

The key objective of both carbon capture, utilization, and storage (CCUS) and well plugging and abandonment (P&A) operations is the formation of secure and stable barriers within the wellbore. Geological CO_2 storage represents a critical technology for mitigating climate change, and sequestering CO_2 in a supercritical state within geological formations effectively prevents its release back into the atmosphere (Zhang and Bachu, 2011). Furthermore, establishing robust and effective barriers is essential to prevent the migration of hydrocarbons into groundwater and the Earth's surface (Vrålstad et al., 2019; Gong et al., 2024; Batista et al., 2021). Such leakage poses significant risks to both ecosystems and human safety. Developing safe and efficient plugging material remains an urgent research priority.

The traditional plugging material in CCUS and P&A operations is cement, which serves the dual purposes of interlayer isolation and wellbore integrity maintenance (Trudel et al., 2019; Laudet et al., 2011; King and King, 2013). However, micro-annuli at the cement-casing interface may form due to shrinkage of the cement matrix, incomplete removal of drilling mud from casing surfaces in plugged well sections, and changes in downhole pressure and temperature (Khalifeh and Saasen, 2020; Genedy et al., 2019). These micro-annuli can create interconnected pathways, allowing trapped fluids from lower well zones to migrate upward into shallower formations or even reach the surface. In deep-water wells, harsh downhole conditions—including high-temperature/high-pressure (HTHP) environments and exposure to acidic and corrosive fluids—degrade conventional cement-based plugs, ultimately undermining zonal isolation (Lu et al., 2023; Ahmed et al., 2020; Kiran et al., 2017).

Cement-based plugging materials are susceptible to corrosion and carbonation degradation under acidic CO_2-rich conditions, particularly in carbon storage applications, which compromises long-term sealing integrity (Mammadov et al., 2025). In complex geological formations, the high viscosity of cement slurries limits

* Corresponding author.
E-mail address: twc18332179810@emails.bjut.edu.cn (W.-C. Tao).
Peer review under the responsibility of China University of Petroleum (Beijing).

https://doi.org/10.1016/j.petsci.2025.11.043

their injectability into intricate wellbores or heterogeneous reservoirs (Fulks et al., 2019). Additionally, conventional cement-based sealing operations require extended setting times, rendering them unsuitable for scenarios demanding rapid sealing (Thorstensen et al., 2022). Despite their widespread use, cement-based materials face persistent critical challenges under extreme CCUS conditions, including, specifically, insufficient long-term sealing reliability, vulnerability to acid-induced degradation, limited injectability, and inflexible setting-time control. These limitations underscore the need for developing novel high-performance alternative materials. Therefore, this study proposes and systematically evaluates a low melting points Sn58Bi alloy as a promising plugging material for CCUS applications.

The Sn58Bi low melting points alloy is a potential cement alternative for CCUS and P&A. The alloy demonstrates slight volumetric expansion during solidification, facilitating metallurgical bonding with casing inner surfaces. The Sn58Bi alloy has a density of 8.7 g/cm^3, excellent flowability in the molten state (>138 °C), and high corrosion resistance to wellbore contaminants like CO_2 and H_2S (Thorstensen et al., 2022; Carragher and Fulks, 2018). Sn58Bi plugs reduce costs compared to cement systems for short-span applications (<5 m), as validated by Zhang et al. (2020a). The Sn58Bi alloy enables a 2-h plug installation versus cement's 72-h curing period, achieving immediate pressure integrity (Thorstensen et al., 2022).

As a conventional plugging material, cement exhibits limited sealing integrity due to its inherent porosity and permeability, often requiring plug intervals of 50–100 m to meet regulatory isolation criteria. In contrast, the Sn58Bi alloy forms a fluid-impermeable barrier through its non-porous crystalline structure, achieving equivalent pressure integrity with 5–10 times shorter plug lengths. Cement is susceptible to chemical degradation in downhole environments, which progressively induces the formation of micro-annular pathways via matrix dissolution. Particularly in carbon storage operations, cement is vulnerable to CO_2 corrosion, resulting in sealing failure due to structural weakening and increased porosity. The Sn58Bi alloy exhibits superior corrosion resistance, especially H_2S and CO_2 (Thorstensen et al., 2022; Carragher and Fulks, 2018). Consequently, it performs better as a carbon-storage plugging material. In addition, when cement is extruded to seal the perforated interval, the cement has poor fluidity and the sealing integrity is not satisfactory (Fulks et al., 2019). The Sn58Bi alloy has good flowability and can infiltrate the perforation holes more easily to achieve effective sealing.

Through an evaluation of the comprehensive performance of Sn58Bi alloy under simulated plugging scenarios for casing, this study demonstrates its potential to significantly reduce CO_2 leakage risks from CO_2 long-term containment systems and abandoned wells, thereby addressing the challenge of inadequate sealing reliability associated with current materials. The findings bridge a key critical research gap in the application of low melting points alloys in CCUS and P&A.

Current research efforts focus on validating the Sn58Bi alloy's technical viability for CCUS/P&A applications while advancing its field implementation in oil and gas well P&A operations. Zhang et al. (2020a, 2020b) quantified the Sn58Bi/rock interfacial strength through standardized shear and tensile testing. They indicated that the bond quality between the Sn58Bi alloy and rock could be enhanced under specific overlying axial pressure conditions. Abdelal et al. (2015) demonstrated that the Sn58Bi alloy generates radial stress during phase-change expansion, significantly enhancing casing/plug friction coefficients. Manataki et al. (2023) observed interfacial microstructure characteristics of Sn58Bi alloy on the contact surface with casing or cement by scanning electron microscopy, and reported no metallurgical bonding between the alloy and steel or cement. In contrast, Hmadeh et al. (2023a, 2023b, 2024a) demonstrated that applying overlying axial pressure significantly enhanced the interfacial bonding quality through controlled radial expansion of Sn58Bi alloy plugs. The application of overlying axial pressure induces radial expansion of the alloy during solidification, thereby enhancing the sealing integrity of the formed alloy plug. Investigation into the influence of overlying axial pressure on the formation mechanism of the alloy plug provides critical insights for guiding the field implementation of Sn58Bi alloy sealing technology and improving its sealing integrity.

Cooling rate significantly affects the microstructure and pore volume fraction of the solidified alloy plug, thereby affecting its mechanical and gas sealing properties (Odaira et al., 2020; Hmadeh et al., 2024c). However, its impact on the expansion behavior of the alloy plug merits further investigation. In engineering applications, enhancing the sealing integrity often involves increasing the length of the plug. Variations in the plug's L/D (specifically through modifying length) are critical for elucidating the relationship between sealing integrity and plug dimensions.

The expansion of Sn58Bi alloy during liquid-solid phase transition is a critical property for its suitability as a plugging material in CCUS and P&A operations. Investigating the expansion process during Sn58Bi alloy plug solidification is essential to optimize sealing integrity. Further research is required to elucidate the solidification behavior of Sn58Bi alloy plugs within casings and the evolution of expansion forces. The expansion behavior during Sn58Bi plug curing is governed by three key parameters: overlying axial pressure, cooling rate, and plugging L/D. In this paper, a specialized test apparatus for alloy plug forming and sealing integrity evaluation was designed. The apparatus melts Sn58Bi alloy via electric heating and solidifies it within the casing to form a sealing plug. Temperature profiles and axial expansion forces were monitored throughout solidification, while the sealing integrity of the formed plug was evaluated using gas pressure testing. Process parameters were systematically varied in the experimental setup: overlying axial pressure (0–2 MPa), plug L/D (2–6), and cooling rates (controlled via air or sand medium). Expansion mechanics during plug formation and gas-sealing performance of consolidated plugs were evaluated across multiple operational variables. This investigation established fundamental insights into the expansion mechanics of Sn58Bi alloy during solidification, providing critical guidance for casing plugging applications in well abandonment operations.

2. Materials and methods

2.1. Materials

The Sn58Bi alloy (58 w.t.% Bi, 42 w.t.% Sn) was selected as the plugging material (produced by Huatai Metals Co., Ltd., China) in this study. Its thermophysical properties are listed in Table 1. The solidification-induced expansion of the Sn58Bi alloy primarily originates from the bismuth constituent—a metal exhibiting volumetric expansion during phase transition. Through strategic alloy design incorporating additional metallic elements, engineers can tailor both melting points (138–271 °C) and expansion coefficients to meet specific downhole requirements. These alloys have low melting points and exhibit conventional thermal expansion-contraction behavior in the solid state. By applying different forming conditions (such as overlying axial pressure), the alloy is forced to undergo radial expansion during formation, thereby forming a tighter bond with the casing. This enhances the sealing integrity of the alloy plug.

Table 1
The properties of Sn58Bi alloys (Zhang et al., 2020a; Hmadeh et al., 2023a).

Properties	Melting point, °C	Surface tension at 155 °C, mPa·s	Thermal expansion coefficient, °C	Volume change (from liquid to solid), %	Density at 21 °C, g/cm^3	Elastic modulus at 21 °C, GPa
Numerical	138	438	1.5×10^{-7}	+0.77	8.72	47.2

The experimental setup utilized N80-grade casing with scaled dimensions (original Ø 177.8 mm × 13.72 mm, reduced by a factor of 3). The inner bore surface roughness was measured as *Ra* 12.5 μm. Relevant mechanical properties are detailed in Table 2.

2.2. Test setup design

The experimental study on casing/Sn58Bi alloy plug formation included expansion force and sealing integrity tests. A schematic diagram of the test apparatus is presented in Figs. 1 and 2. The system consists of several key components: the testing apparatus, a temperature acquisition module, a temperature control box, a pressure acquisition module, a high-pressure pneumatic pump and a computer control system. The testing apparatus comprises a sealing cover, a high-temperature-resistant sealing ring, a casing, sand (as a thermal medium), Sn58Bi alloy, a plexiglas tube, three temperature transducers, a heating rod, a sealing piston, a heat-resistant panel, a pressure transducer, and among other components.

As shown in Fig. 2, the sealing cover connects the upper casing space to the high-pressure pneumatic pump to ensure pressure integrity. The temperature acquisition module (±0.15 °C accuracy, 50 Hz frequency) uses three externally mounted temperature sensor on the casing to record temperatures at the top, middle, and bottom sections of the alloy plug. Owing to the high thermal conductivity of the casing material and the close proximity of the sensors to its outer wall, temperature measurement errors are considered negligible under the experimental conditions. The pressure acquisition module (with an accuracy of ±0.01 MPa and a sampling frequency of 50 Hz) is connected to the sealing piston at the casing base to monitor expansion forces generated by the alloy. The heating rod (700 W power output) operates within a temperature range of 0–500 °C. The heating rod, located in the center of the lower casing section, is used to heat the molten alloy and is connected to a sealing piston and pressure sensor. The cooling rate of the alloy can be adjusted by altering the thermal medium (air or sand) between the casing and the Plexiglas tube. During heating, the sand-filled annular space is uniformly heated alongside the Sn58Bi alloy. Upon cooling, the sand in the annulus provided thermal insulation while facilitating heat transfer. Consequently, in experiments using sand as the thermally conductive medium, the Sn58Bi alloy exhibited a lower cooling rate compared to air cooling. The cooling rate was not measured quantitatively; instead, "fast" and "slow" cooling regimes were produced by adjusting heat-dissipation parameters (e.g., thermal medium type). Additionally, under downhole formation conditions, the alloy plug molding process aligns more closely with sand-cooled scenarios. Increasing the heating temperature of the molten Sn58Bi alloy can reduce its solidification rate.

The working principle of the test apparatus is as follows: As shown in Fig. 2, the alloy is melted using a heating rod, while temperature evolution within the alloy is monitored by sensors mounted externally on the casing. Once the alloy is fully molten, the high-pressure pneumatic pump is activated. Overlying axial pressure (air pressure) is applied through the sealing cover at the upper end of the casing at a rate of 1 MPa/min, with the pressure adjusted between 0 and 2 MPa to ensure experimental safety. After deactivating the heating system, the molten alloy is cooled and

Table 2
The properties of N80 (Jun et al., 2024; Zhang and Wang, 2017).

Properties	Thermal expansion coefficient, °C	Density, g/cm^3	Elastic modulus at 30 °C, GPa	Elastic modulus at 60 °C, GPa	Elastic modulus at 90 °C, GPa
Numerical	1.3×10^{-5}	7.85	196	169	158

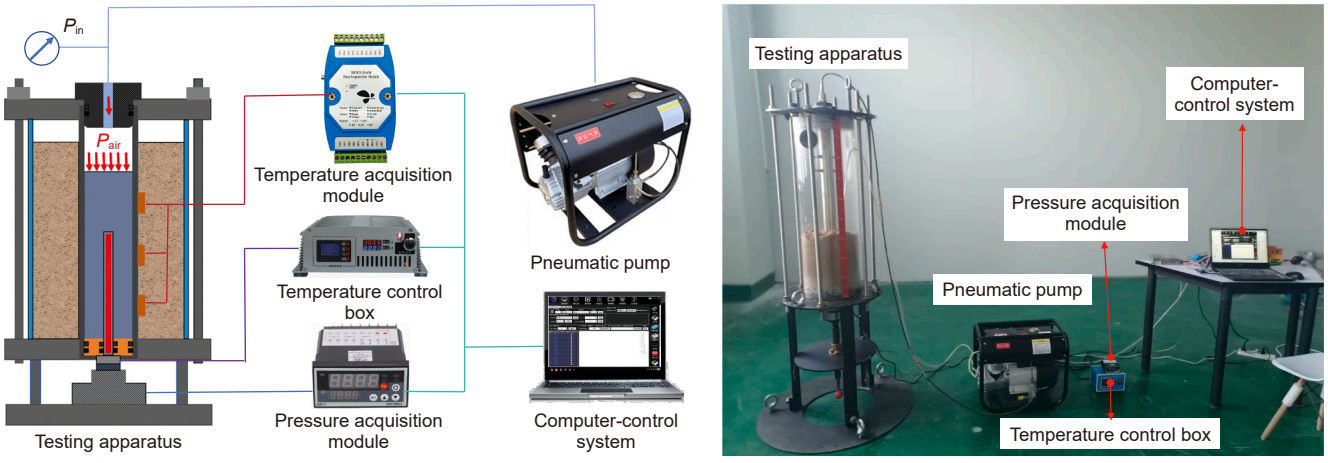

Fig. 1. Schematic and physical diagram of the test apparatus system.

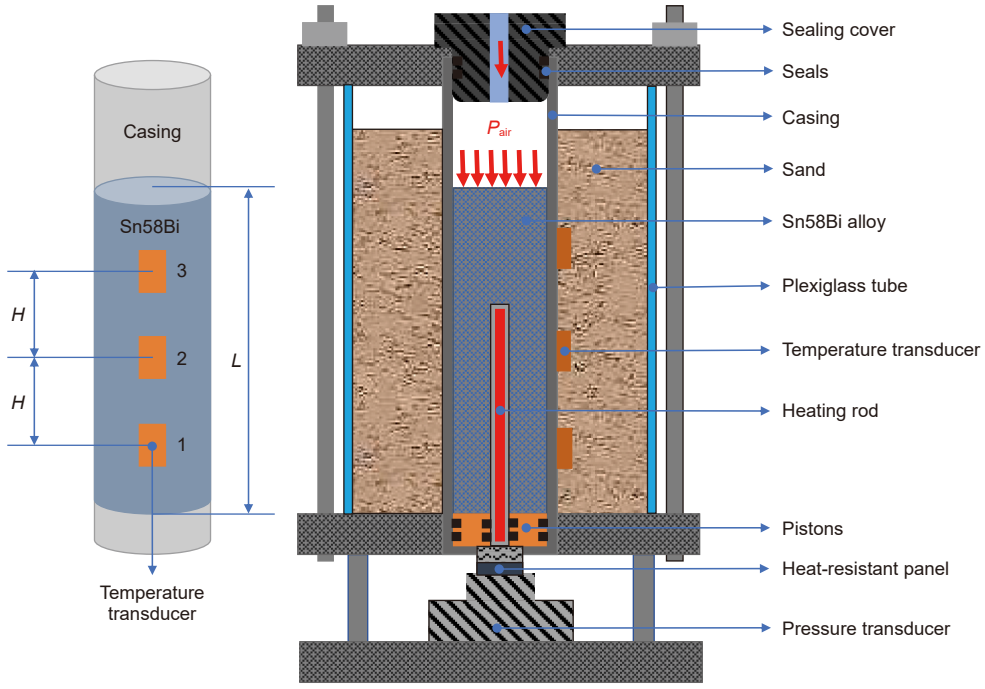

Fig. 2. Testing apparatus.

solidified under the applied overlying axial pressure. The expansion force generated during alloy solidification is recorded by the bottom pressure sensor. Once the alloy plug is fully solidified, the bottom piston is removed, and the end cap is replaced to conduct the gas-sealing test.

3. Experiments and test procedures

To investigate the expansion behavior and solidification process of the Sn58Bi alloy and evaluate the sealing integrity of the resulting plugs under varying forming conditions, the key properties of the Sn58Bi alloy were examined by the research team using the experimental methods summarized in Table 3.

3.1. Reliability and repeatability of the tests

A water-based solution was injected into the casing to validate the test apparatus reliability. As shown in Fig. 3, the internal pressure was elevated to 2 MPa via a high-pressure air pump installed above the solution. The axial pressure was then cyclically adjusted every 30 min (2–1.7 MPa, then back to 2 MPa, and finally reduced to 1.7 MPa) over a 140-min test period. A pressure transducer mounted on the base piston continuously recorded casing pressure fluctuations, with this enabling real-time monitoring of axial pressure dynamics. The strong correlation between the applied axial pressure and the temporal pressure response, as illustrated in Fig. 3, confirmed the reliability of the pressure test unit under controlled conditions.

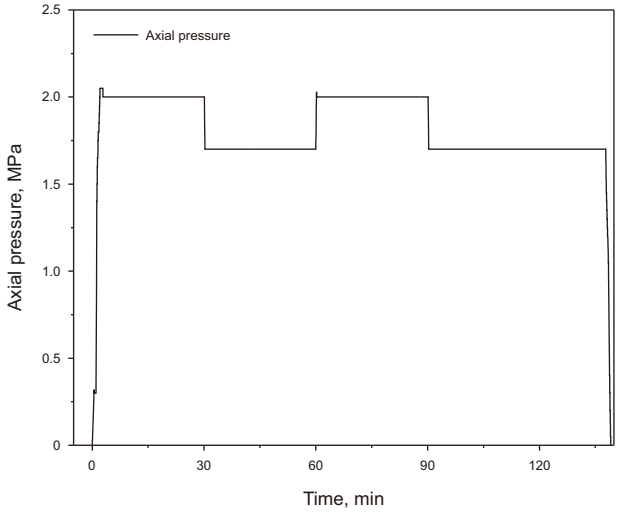

Fig. 3. The apparatus sealing reliability test.

The temperature change during the Sn58Bi alloy plug forming process was monitored by temperature sensors evenly installed throughout the forming apparatus, as shown in Fig. 2. The test procedure was conducted as follows: An appropriate amount of Sn58Bi alloy was heated to 350 °C until fully molten and subsequently injected into the bottom section of the casing. After cooling and solidification into a sealed plug, the alloy was remelted

Table 3
Experiments.

Experiment No.	Experiment name	Objective
EXP-01	Reliability and repeatability of the tests	To validate the rationality and reliability of the designed apparatus
EXP-02	Microstructural analysis	To investigate the effect of overlying pressure on the formation behavior of alloy plugs and analyze the plug formation process
EXP-03	Alloy expansion tests	To investigate the effect of different forming conditions on alloy plug expansion
EXP-04	Sealability tests	To establish the relationship between expansion behavior and sealing performance

in situ under consistent thermal conditions, and relevant temperature data were recorded. To ensure uniform heating and experimental consistency, the entire alloy plug was heated in all subsequent experiments as a whole. The heating bar was activated to melt the alloy, followed by cooling under ambient conditions (using air as the medium).

The temperature evolution of the Sn58Bi alloy, from the heating and melting phases to the solidification phase, is shown in Fig. 4. During the heating of the Sn58Bi alloy, the region of the heating rod that reaches the highest temperatures is located at the upper end of the rod (i.e., at the center of the alloy plug). Consequently, the melting of the Sn58Bi alloy progresses from the center radially outward, with the melting rate at the center being faster than that at the periphery. Upon reaching a temperature of approximately 250 °C, sensor 2 in the center of the alloy plug exhibits a higher temperature than the sensors at the two ends. Additionally, the temperature variations of sensors 1 and 3, distributed symmetrically, are nearly identical. To validate the reproducibility of the temperature experiments, error analysis of the temperature measurements (shown in Fig. 4(b)) was conducted based on three independent sets of measurements. Each test was performed under identical initial and environmental conditions. The maximum standard deviation remained within 6 °C, and all curves exhibited consistent variation trends, confirming the reliability and repeatability of the temperature experimental results.

When the Sn58Bi alloy reaches its melting point, it undergoes a solid-to-liquid phase transition, during which it absorbs a significant amount of heat. As a result, the temperature does not continue to rise, as evidenced by the first plateau (Inflection Point 1) in Fig. 4. Similarly, during solidification, the alloy releases latent heat. Throughout this phase transition, the heat dissipated to the external environment is approximately equal to the heat released by solidification, leading to a period of constant temperature, which is shown as the second plateau (Inflection Point 2) in Fig. 4. The observed temperature profile is consistent with the actual experimental behavior of the Sn58Bi alloy. The time-temperature-phase transition relationship demonstrated in the diagram confirms the reliability of the temperature monitoring system in capturing phase transition characteristics.

3.2. Microstructural analysis

Using the experimental setup shown in Fig. 2, alloy plugs formed under 0 MPa, and 1 MPa overlying pressure together with adjacent casing segments were cross-sectioned. A 10 mm × 10 mm × 10 mm sample was extracted from the interfacial region between the alloy plug and the casing. The sectioned samples were mechanically ground using SiC abrasive paper to expose the alloy-casing interface, followed by ultrasonic cleaning in ethanol. An optical microscope (Keyence VHX-5000, specifications provided in Table 4) was employed to examine the gap at the alloy plug-casing interface on both surface and cross-sectional planes under different overburden pressures, so as to evaluate the effect of pressure on plug integrity. Subsequently, the interfacial region was further divided into upper, middle, and lower segments, each measuring 6 mm × 6 mm × 6 mm. These samples were ground with up to 3000 grit SiC paper, and polished with 1 μm diamond suspension, followed by final polishing with 0.25 μm Al_2O_3 and 0.05 μm SiO_2 suspensions. The interfacial microstructure was then characterized using a field emission scanning electron microscope (FE-SEM, Quanta 650), which was operated at an accelerating voltage of 15 kV.

3.3. Alloy expansion tests

The expansion of the Sn58Bi alloy offers two major advantages: it enhances the interfacial bonding between the alloy plug and the casing, thereby improving pressure resistance; and it minimizes the micro-annulus at the plug-casing interface, thereby enhancing sealing integrity. To quantify the expansion behavior of the alloy during solidification, a customized experimental setup was designed (Fig. 2). As shown in Fig. 5, key parameters affecting the expansion force (σ_e)—including axial pressure (σ_z), cooling rate, ambient temperature, and plug L/D—were systematically evaluated to maximize plugging performance. Additionally, scanning electron microscopy (SEM) analysis of the interfacial microstructure at locations A1 (end), B2 (center), and C3 (end) between the plug-casing reveals a more uniform and refined crystalline grain distribution at the two ends (A1 and C3) after solidification. This can be attributed to the faster cooling and solidification rates at the end regions compared to the center of the plug. Consequently, as the ends solidify first, the highest solidification-induced expansion force is generated in the central region of the alloy plug.

Increasing the L/D (with the diameter fixed, which alters only the sealing length) has two effects: (1) improving the alloy plug's sealing integrity by extending the sealing length, and (2) when the plug length is sufficient, preferential solidification occurs at the top and bottom ends (due to rapid heat dissipation—via contact

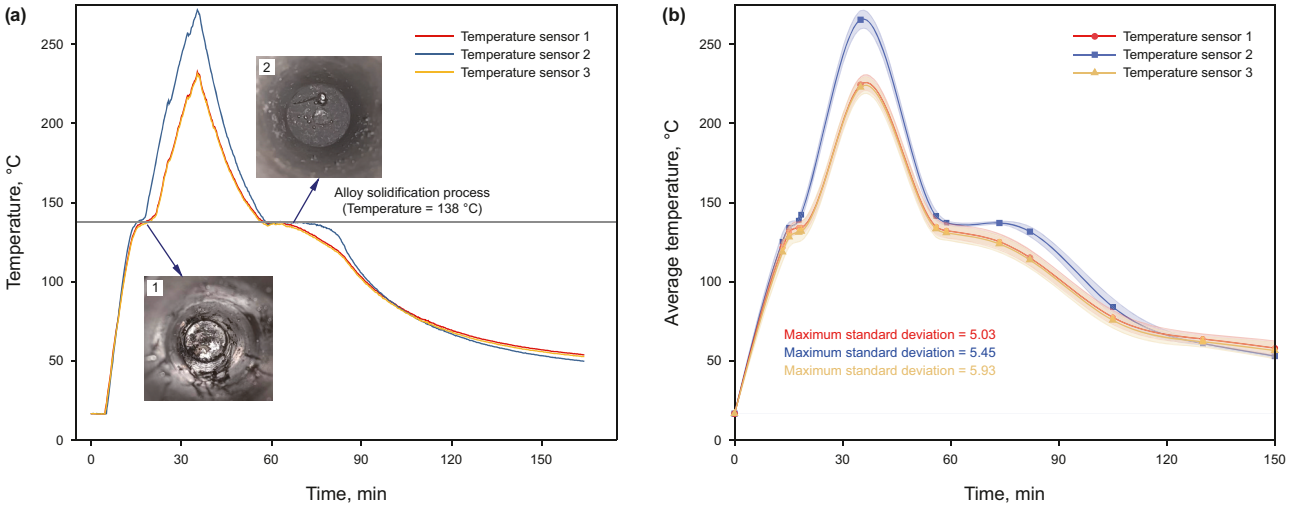

Fig. 4. Temperature change during melting and solidification of the Sn58Bi alloy plugs.

Table 4
Specifications of the VHX-5000.

Characteristic	Image sensor	Virtual pixels	Frame rate	Magnification
Specification	1/1.8 inch	1600 (H) × 1200 (V)	0–50 fps	0–100

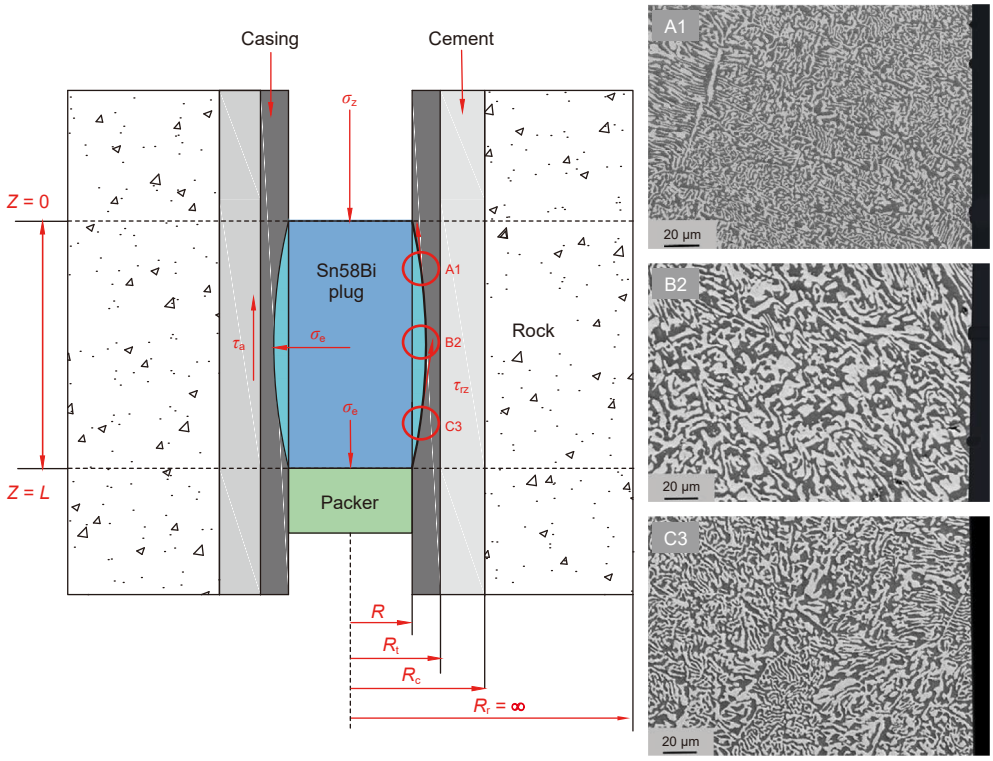

Fig. 5. Expansion stress distribution in the Sn58Bi alloy plugs.

with air/water at the top and the packer at the bottom) forces the middle alloy to expand radially during solidification, thereby enhancing sealing integrity. The cooling rate (e.g., sand cooling vs air cooling) influences the entire alloy plug formation process, including: (1) the duration of gas escape from the molten alloy during solidification, (2) the expansion pattern during solidification. For instance, faster heat dissipation at the casing interface causes the alloy adjacent to the mold to solidify first, leading to axial expansion and reduced sealing integrity.

To measure the magnitude of the expansion force generated by the Sn58Bi alloy during the expansion process, the bottom axial expansion force during the solidification process of the Sn58Bi alloy was recorded using the pressure transducer at the bottom of the test setup in Fig. 2. The test procedure is as follows.

(a) Prepare casing (N80, 59.27 mm × 4.57 mm) with a plugging length of L that matches the volume for Sn58Bi alloy.
(b) The experimental setup is assembled with the casing securely installed according to the specified procedure.
(c) A predetermined amount of Sn58Bi alloy was heated to 350 °C in a furnace until fully molten and subsequently injected into the casing. The alloy was then allowed to cool and solidify in situ to form a sealing plug.
(d) Turn on the heating equipment, adjust the temperature of the heating rods, record the temperature transducer data, and check the temperature transducer position and readings.
(e) After calibrating the test data, inject the thermal conductivity medium from the side hole of the test apparatus to fill around the casing. Dry the sand to eliminate water interference. For the natural air-cooled group, do not add any additional thermal medium.
(f) Start the heating equipment and adjust the temperature of the heating rod to 250 °C. Wait until the Sn58Bi alloy is completely melted. Observe the temperature change; stop heating when the temperature exceeds the alloy's melting point (confirmed by complete melting).
(g) Use a pneumatic pump to apply overlying axial pressure (0–2 MPa). Increase the pressure gradually and stop when the sensor reading reaches the set value.
(h) Record temperature and pressure transducer data trends over time at different cooling rates.
(i) To complete the test, change the test conditions (overlying axial pressure, plugging L/D, and ambient heat transfer medium) and repeat steps c to g to collect comprehensive data.

3.4. Sealing integrity tests

Samples of the Sn58Bi alloy plug-casing interface produced under varying forming conditions were obtained through expansion behavior tests. To establish the relationship between the alloy's expansion behavior and the gas sealing integrity of its plugs, a sealing test was conducted alongside each expansion test procedure. This is essential to determine the gas breakthrough pressure values of the plugs. The Sn58Bi alloy plug exhibits gradual expansion after solidification—a process that persists for up to one

month (Hmadeh et al., 2024b). To evaluate the sealing integrity resulting from short-term expansion of the alloy plug immediately after formation, after the Sn58Bi alloy plugs were cooled and solidifying for 5 h, the samples were evaluated for their gas sealing integrity. The apparatus used for this assessment is shown schematically in Fig. 6. The test procedure is as follows.

(a) After the expansion test, the Sn58Bi alloy plug-casing composite plugs are cooled for several hours (refer to the schematic diagram in Fig. 6).
(b) The gas pressure pipeline is connected to the high-pressure pneumatic pump at the base of the testing apparatus, which served as the source of high-pressure gas (air at room temperature). The gas pressure was gradually increased to the set pressure (0–30 MPa) and maintained for 30 min.
(c) If fluctuations in the gas pressure transducer's readings at the top of the apparatus are observed, a sealing failure can be inferred. If no leakage is detected, the gas pressure at the bottom end of the Sn58Bi alloy plug will increase until breakthrough occurs (i.e., the pressure at which gas penetrates the alloy plug and starts leaking), at which point the breakthrough pressure is recorded.
(d) The breakthrough pressure is recorded, and the test results are analyzed.

4. Results and discussion

4.1. Effect of overlying axial pressure

When cooled in an unconstrained manner during solidification, the Sn58Bi alloy plugs underwent most of their expansion in unconstrained directions. In this experiment, the molten Sn58Bi alloy was subjected to radial and axial bottom-end constraints via a piston. As shown in Fig. 8(a), in the absence of applied overlying axial pressure, the dominant expansion during solidification was in the axially (upward) direction. Consequently, the Sn58Bi alloy plug formed a small protuberance at its tip (Fig. 8(a)), while the pressure transducer at the plug base showed no pressure fluctuations. The results confirmed that Sn58Bi alloy expansion during cooling predominantly occurred in unconstrained directions. During solidification, an overlying axial pressure was exerted on the upper axial end of the Sn58Bi alloy plug. This resulted in more radial expansion and bottom-end axial expansion during solidification, and the radial expansion could effectively enhance the sealing integrity. Fig. 8 illustrates the forming process of Sn58Bi alloy plugs (200.52 mm in length) under three distinct overlying axial pressures.

The alloy was heated above its melting point and then air-cooled. The Sn58Bi alloy plug forming process comprised three phases: molten liquid → semi-solid (paste) → solid. Expansion forces were generated during the semi-solid phase because the alloy expanded as it solidified. Following solidification, the plug underwent volumetric shrinkage. Temperature transducers recorded that the solidification rate at both ends of the plugs exceeded that of the central region. As shown in Fig. 7, the expansion force developed radially outward from the plug center during solidification.

Applying overlying axial pressure restricted upward expansion (Fig. 9). Under higher axial pressures, greater expansion forces were measured at the plug base (e.g., 0.1 MPa at 1 MPa axial pressure, and 0.15 MPa at 2 MPa axial pressure). Gas sealing testing of the formed Sn58Bi plugs (Fig. 8(d)) revealed that increasing the overlying axial pressure reduced the probability of gas leakage through the plug. The sealability of the Sn58Bi alloy plugs increased linearly with applied overlying axial pressure.

After forming Sn58Bi alloy plug-casing samples under overlying axial pressure, interfacial gap size distribution between the Sn58Bi plug and casing was examined via microscopy, as shown in Fig. 9. Interfacial bonding was enhanced and gap size was reduced under axial pressure. Microscopy indicated that overlying axial pressure promoted radial expansion at the interface, improving sealing integrity.

The application of overlying axial pressure during alloy plug formation significantly enhances sealing integrity. The required overlying axial pressure for sealing integrity can be naturally supplied by downhole conditions during operations. Hydrostatic pressure—approximately 1 MPa per 100 m—from the casing water column acts on the plug, producing a mechanical effect equivalent to that of externally applied axial pressure in laboratory settings, thereby generating effective axial stress downhole to improve sealing integrity. This eliminates the need for additional tools to

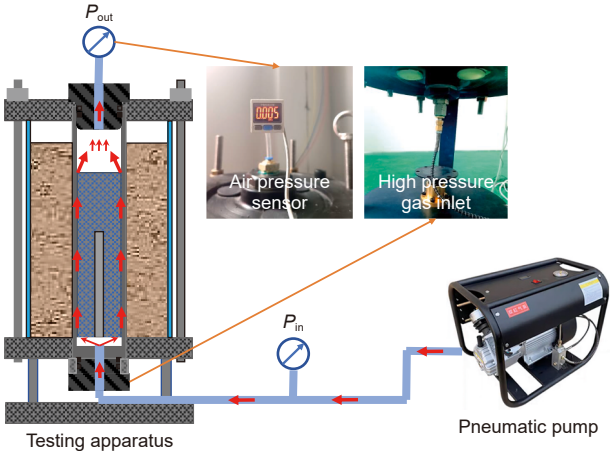

Fig. 6. Schematic diagram of sealing integrity testing apparatus.

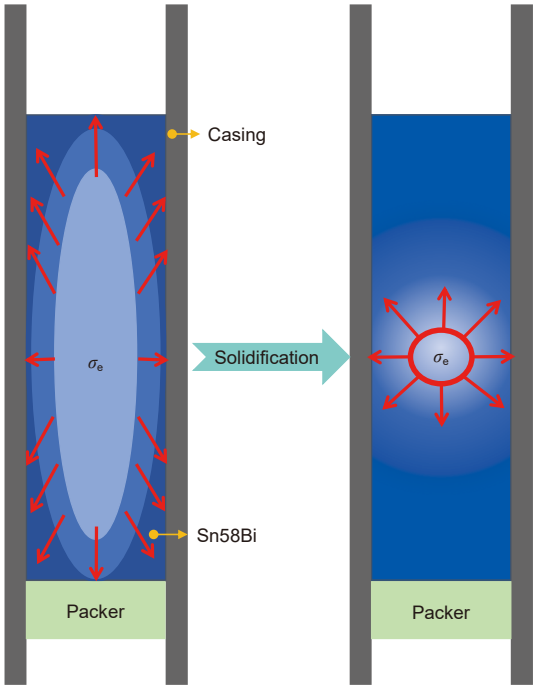

Fig. 7. Solidification and expansion process of the Sn58Bi alloy plugs.

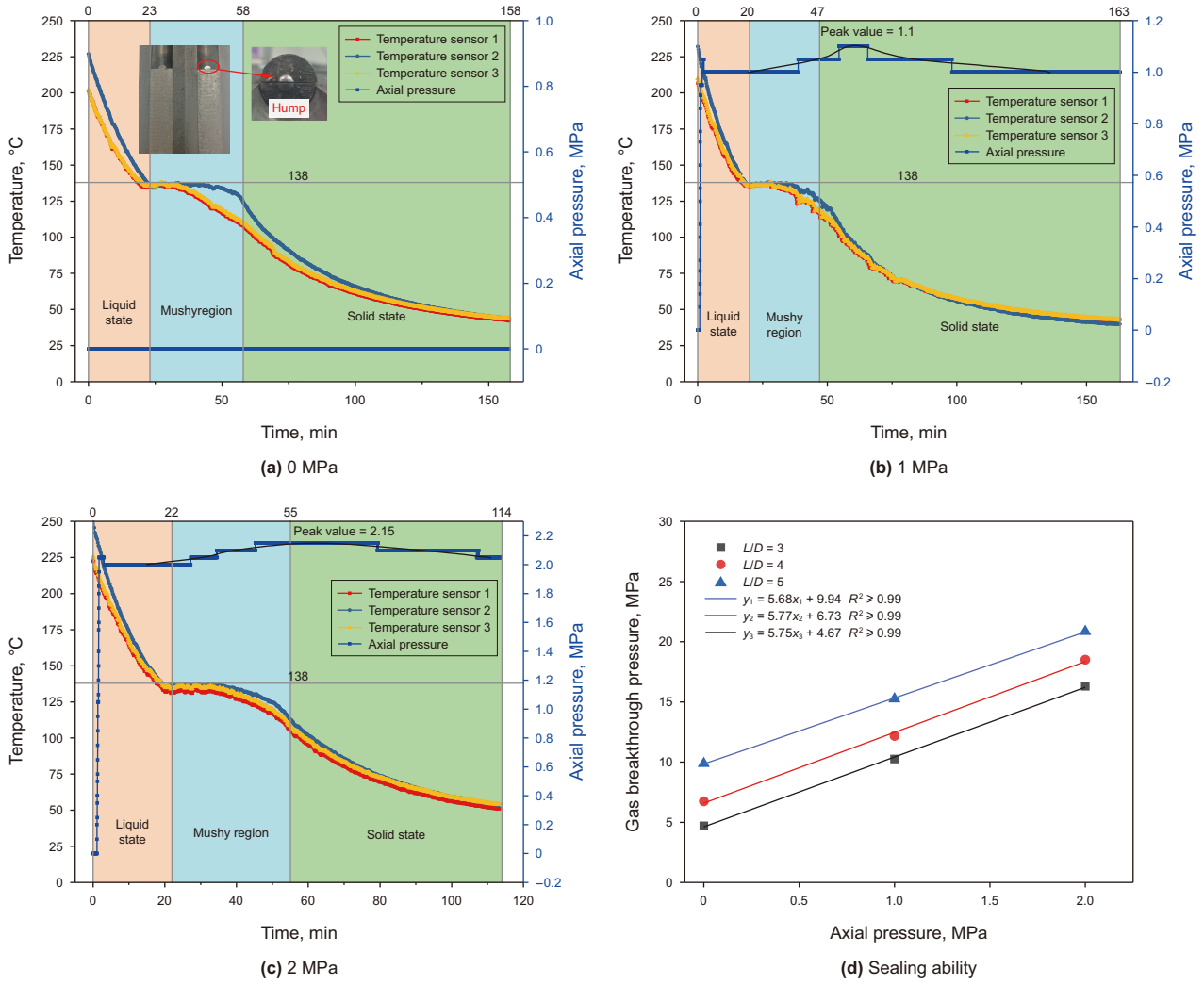

Fig. 8. Change of expansion force during solidification of alloy plugs under different overlying axial pressures and sealability after forming.

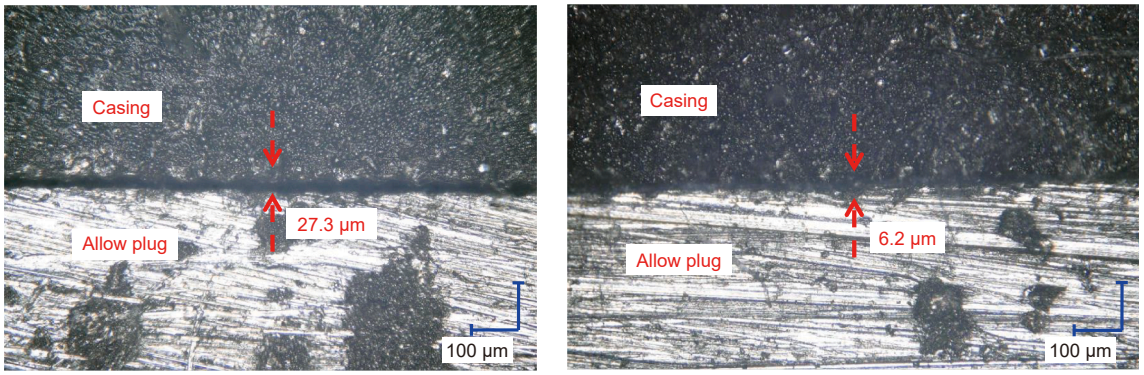

Fig. 9. The interface gap of Sn58Bi alloy plug-casing change with the overlying axial pressure.

generate axial force, simplifying operational procedures. Consequently, the dosage of alloy material can be optimized based on sealing requirements and corresponding hydrostatic pressures at different well depths, ensuring reliability while reducing material costs.

4.2. Effect of cooling rates

The expansion behavior of Sn58Bi alloy plugs varies with cooling rates. Extended solidification time increases expansion duration, enhancing sealing integrity (Hmadeh et al., 2024a). To

investigate the relationship between cooling rate and Sn58Bi alloy plug performance during forming and simulate forming at the well bottom, experiments were conducted by altering conditions for 200.52-mm plugs: a) axial pressures, b) cooling media (air or sand). Results are shown in Fig. 10. During cooling, sand surrounding the casing acted as a heat buffer, slowing heat dissipation to ensure uniform cooling. This dual role prolonged the alloy's cooling process (Fig. 10(b)). As shown in Fig. 11, under sand-cooling conditions, the maximum difference in cooling rate within the mushy zone (i.e., the solid-liquid coexistence region) of the alloy plug was 0.08 °C/min, with a maximum temperature difference of 4 °C. In contrast, air-cooling resulted in a maximum cooling rate difference of 0.19 °C/min and a maximum temperature difference of 11.9 °C. The sand-cooling method exhibited a slower and more uniform cooling profile than air-cooling. This slower, more uniform cooling resulted in higher expansion forces, leading to improved sealing integrity of the formed Sn58Bi alloy. The objective of the gas-seal test was to ascertain the impact of the two distinct cooling conditions on the sealing integrity of Sn58Bi alloy plugs. As shown in Fig. 12, sealability under sand-cooling conditions was significantly higher than that under air-cooling conditions.

Analysis of Figs. 11 and 12 indicates that the sealing integrity improves with extended solidification time under both cooling conditions, with an average improvement rate of 2.34 MPa per 10 min. Prolonged solidification time enhances the final sealing integrity of the formed alloy plug. Sufficient solidification time promotes the escape of internal gases in the plug, while uniform cooling prevents the formation of defects such as pores and cracks, defects that commonly occur during rapid solidification processes. Although a direct cost-benefit analysis was not included, the experimental data reveal critical optimization pathways. Future work will involve developing a detailed cost model to quantify the global optimum of sealing performance-cost balance under time and material constraints.

Given the uncontrollable nature of the bottom-hole environment, the cooling rate can be controlled by adjusting the preheating temperature. Current heating methods include electric heating and thermite heating (a method using thermite reaction for heat release; Abdelal et al., 2024). Thermite heating achieves

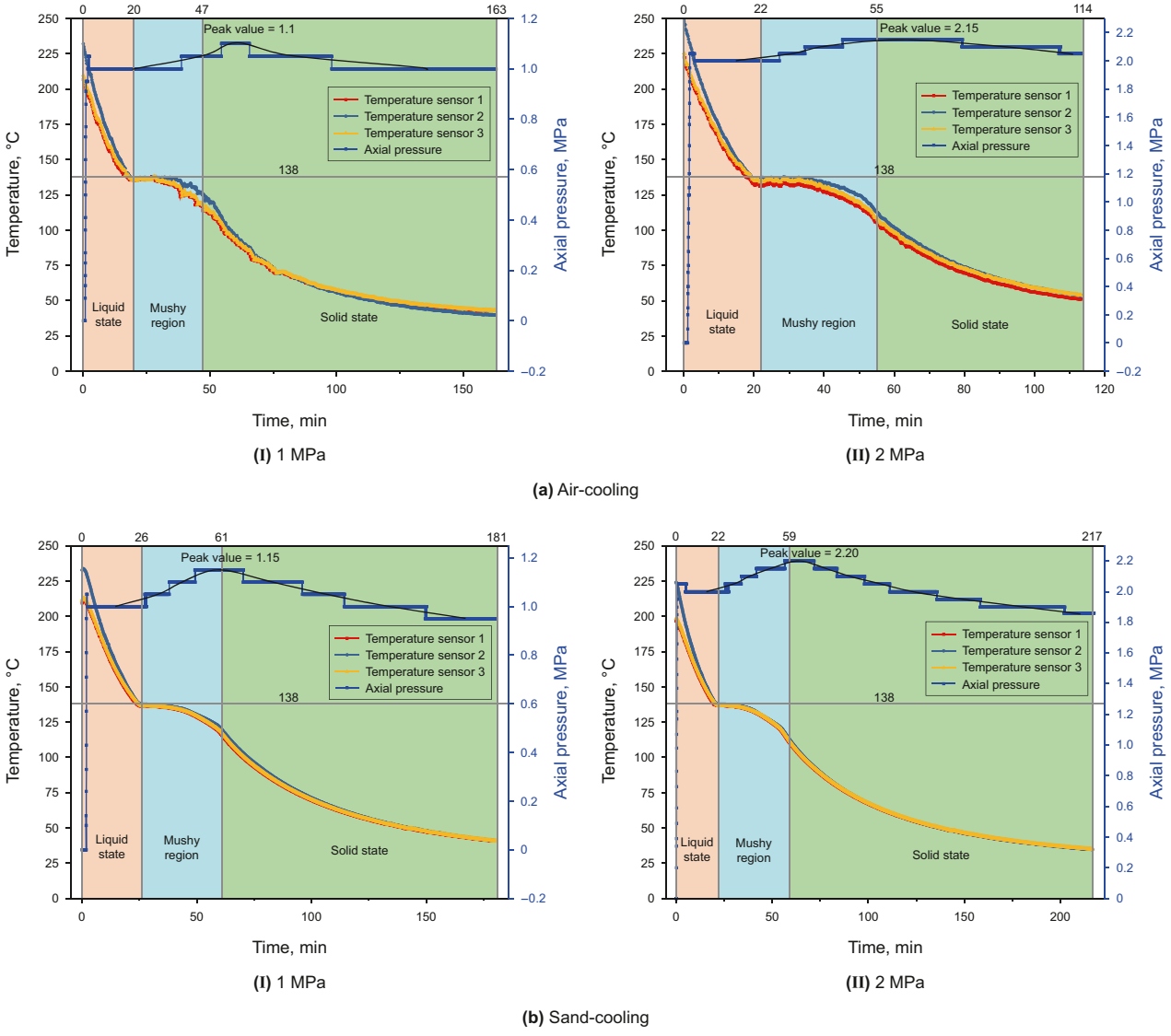

Fig. 10. Change of expansion force under the condition that the heat-conducting medium is air and sand.

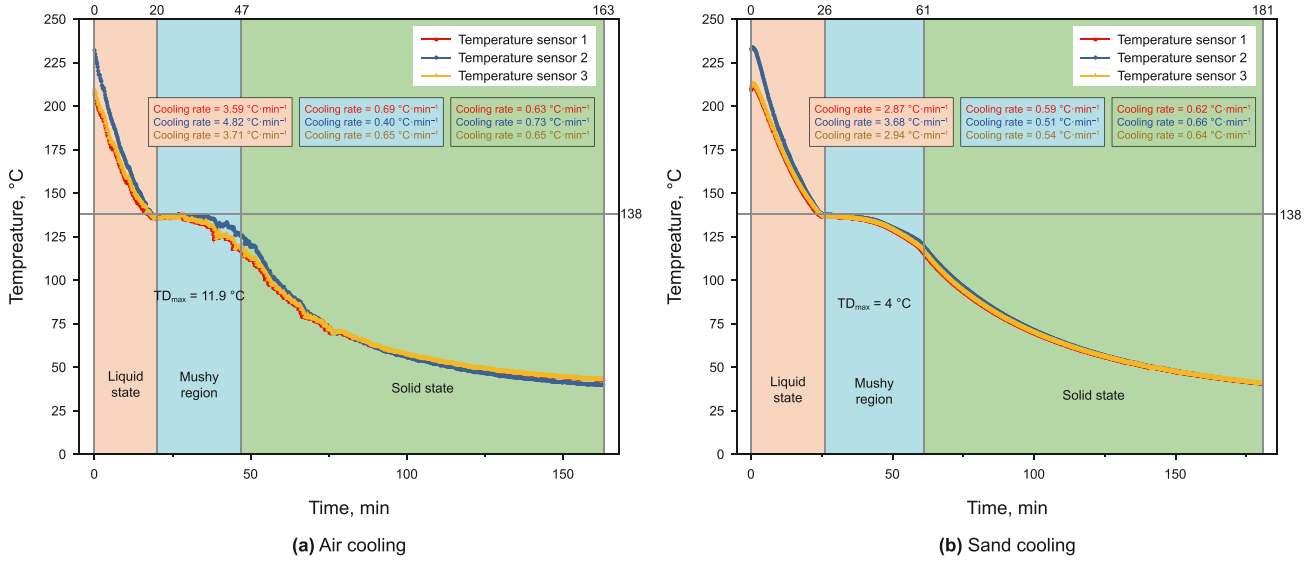

Fig. 11. Temperature variation during alloy plug formation under different cooling conditions.

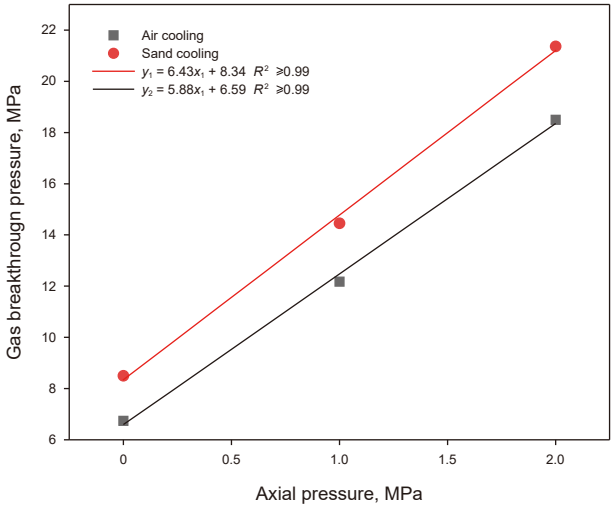

Fig. 12. Sealability of Sn58Bi alloy under different cooling conditions.

higher temperatures, enabling rapid alloy heating. In contrast, electric heating systems experience significant energy losses during power transmission, which may increase operational costs for elevating the alloy's temperatures. Therefore, proper regulation of the heating temperature and duration is critical to prevent sealing defects that are induced by rapid cooling while maintaining cost efficiency.

4.3. Effect of L/D

For cement plugs, increasing plug length typically enhances sealing integrity. It is critical to investigate the effect of the *L*/*D* of the Sn58Bi alloy plugs on the sealing integrity. Further research is required to elucidate the influence of the *L*/*D* on expansion behavior. During Sn58Bi alloy plug forming, the contact interface with the casing solidifies prematurely, with the solidification front expanding toward the center. In this study, expansion during solidification predominantly occurs in unrestricted directions, including the axial direction and the region of molten Sn58Bi alloy, continuing until complete solidification is achieved. The variation in expansion force during forming of Sn58Bi plugs with three *L*/*D* (*L*/*D* = 3, 4, and 5) under 1 MPa axial pressure is shown in Fig. 13. This variation was achieved solely by adjusting plug length while keeping the diameter constant.

As shown in Fig. 13, the peak axial expansion force initially increases and then decreases to zero with increasing *L*/*D*. During solidification of the molten alloy at the center, volume expansion of the alloy generates an outward radial force. If the alloy at the axial ends solidifies first, the subsequent solidification of the central region directs the expansion radially (Hmadeh et al., 2023a). Fig. 13(a) and (b) indicate that increasing the *L*/*D* (e.g., *L*/*D* = 4) enhances axial expansion. Shorter Sn58Bi alloy plugs exhibit faster and more uniform cooling rates, leading to nearly simultaneous solidification at the center and axial ends, which induces measurable axial displacement of the alloy plug. When the *L*/*D* exceeds 5, no axial-end expansion force is detected during solidification. Consequently, the solidified alloy at both ends restricts axial expansion of the central region, resulting in predominant radial expansion and improved sealing integrity.

As shown in Fig. 13(c), the contact pressure between the Sn58Bi alloy and the pressure transducer at the piston interface varied with temperature. This relationship is further illustrated in Fig. 13(d). After the Sn58Bi alloy plug solidified and formed, thermal contraction reduced the contact pressure at the Sn58Bi alloy-metal piston interface as temperature decreased. Consequently, the temperature-dependent expansion force of the Sn58Bi alloy plug in the solid state was quantified. In downhole sealing operations, sealing performance is directly correlated with the expansion force of the Sn58Bi alloy. Experimental results indicated that the expansion force increased with increasing temperature. Because of in-situ creep, performance deteriorated markedly at temperatures >60 °C; therefore, Sn58Bi is recommended for service conditions ≤60 °C (Hmadeh et al., 2024b).

As shown in Fig. 14, the influence of the *L*/*D* of Sn58Bi alloy plugs on the sealing integrity was investigated through gas sealing tests. Fig. 14 indicates the variation in sealability of Sn58Bi alloy plugs with *L*/*D* under three distinct overlying axial pressure conditions, showing a consistent upward trend across all pressures. The sealability of Sn58Bi alloy plugs showed a marked increase as

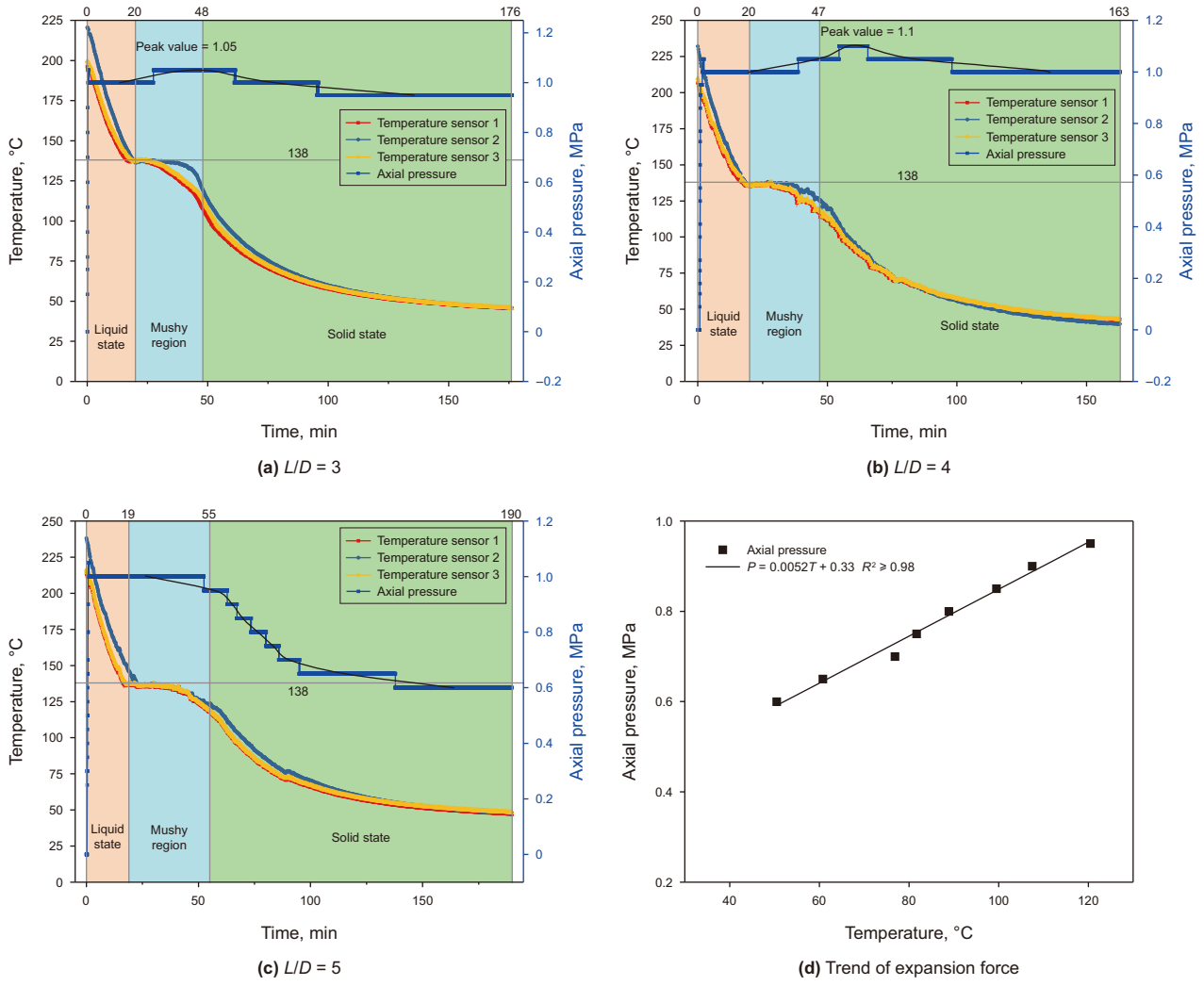

Fig. 13. Variation process of expansion force under different plugging lengths.

the L/D increased. This trend was particularly pronounced under zero overlying axial pressure conditions.

The accelerated heat dissipation at the upper and lower ends of the alloy plug (attributed to conductive heat transfer and thermal exchange with adjacent media such as air, water, and packer components) promotes preferential solidification at these regions. This localized solidification forces the central molten alloy to expand radially during cooling, thereby enhancing sealing

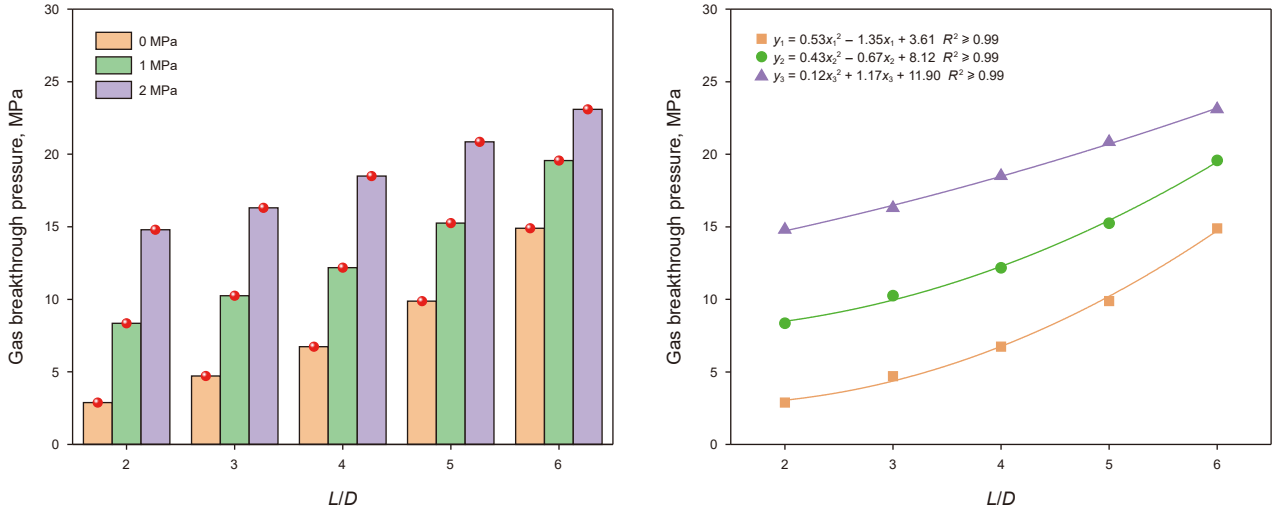

Fig. 14. Sealability of the Sn58Bi alloy plugs with different L/D.

integrity. Experimental results indicate that when the *L*/*D* of the alloy plug exceeds 5, the radial expansion of Sn58Bi alloy plugs at the casing-plug interface becomes significantly more pronounced during the solidification process, which leading to improved sealing integrity. Consequently, in field operations, rapid solidification at both ends of the alloy plug (compared to the central section) can be achieved by either optimizing the downhole *L*/*D* to values greater than 5 or implementing targeted cooling measures on the alloy plug ends to maximize plug's sealing integrity.

5. Conclusions

This study investigated the expansion behavior of Sn58Bi low melting points alloy for downhole casing plugging during solidification. A specialized test apparatus was designed to analyze the alloy's expansion behavior, temperature-expansion force response, and post-solidification gas sealing integrity under the following conditions: three overlying axial pressures (0 MPa, 1 MPa, and 2 MPa), two cooling media (air and sand), and varying *L*/*D*. Experimental results indicated the feasibility of Sn58Bi alloy as a reliable casing plugging material. The alloy's plugging performance was further validated under diverse operational scenarios, providing critical insights for developing high-performance downhole casing plugging agents. Key conclusions are summarized below.

(a) Applied overlying axial pressure effectively enhances radial expansion during plug formation. Under an overlying axial pressure of 1 MPa, the ring gap at the interface between the alloy plug and the casing decreased from 27.3 μm (0 MPa) to 6.2 μm (1 MPa). Within the overlying axial pressure range of 0–2 MPa, sealing integrity among three groups with different plug *L*/*D* indicated improved sealability of the alloy plugs. The sealing integrity increased by an average of 5.73 MPa per 1 MPa increase in overlying axial pressure. During plugging operations, radial expansion of the alloy can be induced by applying overlying pressure, forming an alloy plug with enhanced sealing integrity. Simultaneously, material costs are reduced while the sealing requirements are met.

(b) To prevent defects, the molten alloy must be maintained at a temperature high enough to avoid rapid cooling upon contact between the molten alloy and the casing at the well bottom. Inadequate temperature retention of the molten alloy shortens the interfacial gas escape time, potentially leading to the formation of defects such as voids, or cracks during solidification. Reducing the solidification rate of Sn58Bi alloy plugs and improving cooling uniformity during the solidification process can enhance both axial compressive force and radial expansion force. These improvements optimize the structural integrity of the plugs, directly resulting in improved gas sealing integrity.

(c) In plugging operation, sealing integrity can be effectively improved by increasing the *L*/*D* of Sn58Bi alloy plug (achieved solely by increasing length while keeping the diameter constant). When the *L*/*D* exceeds 5 (experimental threshold), both ends of the plug undergo heat dissipation while exchanging heat with adjacent thermally conductive media (e.g., air, water, and packer components). The axial ends solidify first. During solidification of the central region, axial expansion is constrained by the solidified ends, resulting in enhanced radial expansion and improved sealing integrity. Accelerating the solidification of the plug's axial ends can enhance gas-tight sealing integrity.

(d) In plugging operations, the sealing integrity of the Sn58Bi alloy plug increases proportionally with its radial expansion. Experimental data indicate that the radial expansion force is enhanced by increasing temperature. Based on in situ creep behavior, the optimal downhole temperature for achieving maximum sealing performance is 60 °C.

CRediT authorship contribution statement

Chun-Qing Zha: Data curation, Conceptualization. **Gong-Hui Liu:** Investigation, Funding acquisition, Formal analysis. **Wei Wang:** Project administration, Methodology.

Declaration of competing interest

The authors declare that they have no known competing financial interests or personal relationships that could have appeared to influence the work reported in this paper.

Acknowledgement

The research was supported by the Natural Science Foundation of China (contract No. U23B2081).

References

Abdelal, G.F., Robotham, A., Carragher, P., 2015. Numerical simulation of a patent technology for sealing of deep-sea oil wells using nonlinear finite element method. J. Pet. Sci. Eng. 133, 192–200. https://doi.org/10.1016/j.petrol.2015.05.010.

Abdelal, G.F., Carragher, P., Clark, B., 2024. Investigating creep performance of Wellok BiSN plug for sealing of offshore wells. Geoenergy Sci. Eng. 242, 213153. https://doi.org/10.1016/j.geoen.2024.213153.

Ahmed, S., Salehi, S., Ezeakacha, C., 2020. Review of gas migration and wellbore leakage in liner hanger dual barrier system: challenges and implications for industry. J. Nat. Gas Sci. Eng. 78, 103284. https://doi.org/10.1016/j.jngse.2020.103284.

Batista, W.G.S., Costa, B.L.S., Aum, P.T.P., et al., 2021. Evaluation of reused polyester resin from PET bottles for application as a potential barrier material. J. Pet. Sci. Eng. 205, 108776. https://doi.org/10.1016/j.petrol.2021.108776.

Carragher, P., Fulks, J., 2018. A new look at sealing with bismuth and thermite. In: SPE Annual Technical Conference and Exhibition, Dallas, Texas, USA. https://doi.org/10.2118/191469-MS.

Fulks, J., Carragher, P., Prapoo, H., 2019. Bismuth abandonment plugs: the possibilities are endless. In: SPE Symposium: Decommissioning and Abandonment. Kuala Lumpur, Malaysia. https://doi.org/10.2118/199228-MS.

Genedy, M., Matteo, E.N., Stenko, M., et al., 2019. Nanomodified methyl methacrylate polymer for sealing of microscale defects in wellbore systems. J. Mater. Civ. Eng. 31 (7), 04019118. https://doi.org/10.1061/(ASCE)MT.1943-5533.0002754.

Gong, P., Fu, H.C., He, D., et al., 2024. Novel material to enhance the integrity of CCUS cement sheath: exploration and application of calcium aluminate cement. Geoenergy Sci. Eng. 124, 205247. https://doi.org/10.1016/j.jgsce.2024.205247.

Hmadeh, L., Elahifar, B., Sangesland, S., 2023a. The sealing behavior of bismuth-based metal plugs. In: ASME 2023 42nd International Conference on Ocean, Offshore and Arctic Engineering. Volume 9: Offshore Geotechnics; Petroleum Technology. Melbourne, Australia. https://doi.org/10.1115/OMAE2023-104309.

Hmadeh, L., Elahifar, B., Sangesland, S., et al., 2023b. A full laboratory Study on the physical and mechanical properties of a bismuth plug. In: SPE/IADC International Drilling Conference and Exhibition. Stavanger, Norway. https://doi.org/10.2118/212561-MS.

Hmadeh, L., Manataki, A., Jaculli, M.A., et al., 2024a. A sealability study on bismuth-tin alloys for plugging and abandonment of Wells. SPE J. 29 (7), 3500–3515. https://doi.org/10.2118/219744-pa.

Hmadeh, L., Jaculli, M.A., Vedvik, N., et al., 2024b. The effect of temperature on the sealability of bismuth–tin alloy plugs. Geoenergy Sci. Eng. 241, 213107. https://doi.org/10.1016/j.geoen.2024.213107.

Hmadeh, L., Manataki, A., Jaculli, M.A., et al., 2024c. Mitigating gas migration with eutectic bismuth alloy plugs. Pet. Res. 10 (2), 331–341. https://doi.org/10.1016/j.ptlrs.2024.09.003.

Jun, J., Shan, H.B., Zhu, X.H., et al., 2024. The effect of string mechanical properties degradation on wellhead growth of offshore HPHT wells. Petrol. Sci. Technol. 42 (19), 2608–2632. https://doi.org/10.1080/10916466.2023.2180035.

Khalifeh, M., Saasen, A., 2020. Introduction to Permanent Plug and Abandonment of Wells. Springer Nature. https://doi.org/10.1007/978-3-030-39970-2.
King, G.E., King, D.E., 2013. Environmental risk arising from well-construction failure–differences between barrier and well failure, and estimates of failure frequency across common well types, locations, and well age. SPE Prod. Oper. 28, 323–344. https://doi.org/10.2118/166142-MS.
Kiran, R., Teodoriu, C., Dadmohammadi, Y., et al., 2017. Identification and evaluation of well integrity and causes of failure of well integrity barriers (A review). J. Nat. Gas Sci. Eng. 45, 511–526. https://doi.org/10.1016/j.jngse.2017.05.009.
Laudet, J.B., Garnier, A., Neuville, N., et al., 2011. The behavior of oil well cement at downhole CO_2 storage conditions: static and dynamic laboratory experiments. Energy Proc. 4, 5221–5258. https://doi.org/10.1016/j.egypro.2011.02.504.
Lu, Y.X., Spencer-Williams, I., Chang, N., et al., 2023. Experimental study of genesis of a geologically activated and self-sealing cementing material for deep wellbore plugging and abandonment under acidic conditions. Geoenergy Sci. Eng. 221, 111299. https://doi.org/10.1016/j.petrol.2022.111299.
Mammadov, O., Mahmoud, A.A., Al-Yaseri, A., et al., 2025. A comprehensive review of cement degradation analysis under downhole conditions: CCS/CCUS/CO_2-EOR applications. ACS Omega 10 (27), 28515–28533. https://doi.org/10.1021/acsomega.4c11295.
Manataki, A., Kontis, P., Sangesland, S., 2023. Investigation of the microstructure of bismuth alloy and its interaction with cement and steel casing. In: SME 2023 42nd International Conference on Ocean, Offshore and Arctic Engineering. Volume 9: Offshore Geotechnics; Petroleum Technology. Melbourne, Australia. https://doi.org/10.1115/OMAE2023-103843.
Odaira, N., Fujiwara, T., Arita, Y., 2020. Behavior of lead-bismuth eutectic (LBE) expansion caused by phase transition in response to heat treatment. Nucl. Eng. Des. 365, 110714. https://doi.org/10.1016/j.nucengdes.2020.110714.
Thorstensen, E., Vadset, K., Straume, M.K., et al., 2022. Bismuth plugs used to cap all Wells during the final phase of the valhall DP abandonment campaign, offshore Norway. In: OTC (Offshore Technology Conference)Houston, Texas, USA. https://doi.org/10.4043/31897-MS.
Trudel, E., Bizhani, M., Zare, M., et al., 2019. Plug and abandonment practices and trends: a British Columbia perspective. J. Petrol. Sci. Eng. 183, 106417. https://doi.org/10.1016/j.petrol.2019.106417.
Vrålstad, T., Saasen, A., Fjær, E., et al., 2019. Plug & abandonment of offshore wells: ensuring long-term well integrity and cost efficiency. J. Petrol. Sci. Eng. 173, 478–491. https://doi.org/10.1016/j.petrol.2018.10.049.
Zhang, H., Ramakrishnan, T.S., Elias, Q.K., et al., 2020a. Evaluation of bismuth-tin alloy for well plug and abandonment. SPE Prod. Oper. 35 (1), 111–124. https://doi.org/10.2118/199363-PA.
Zhang, H., Ramakrishnan, T.S., Magdy Elkady, Youssef, et al., 2020b. Comparative evaluation of bismuth-silver and bismuth-tin alloys for plug and abandonment. SPE Drill. Complet. 36 (2), 368–382. https://doi.org/10.2118/202488-PA.
Zhang, M., Bachu, S., 2011. Review of integrity of existing wells in relation to CO_2 geological storage: what do we know. Int. J. Greenh. Gas Control 5 (4), 826–840. https://doi.org/10.1016/j.ijggc.2010.11.006.
Zhang, Z., Wang, H., 2017. Effect of thermal expansion annulus pressure on cement sheath mechanical integrity in HPHT gas wells. Appl. Therm. Eng. 118, 600–611. https://doi.org/10.1016/j.applthermaleng.2017.02.075.